LAWRENCE
LIVERMORE
NATIONAL
LABORATORY

LLNL-CONF-843036

Correcting energy estimation errors due to finite sampling of transition edge sensor data

M. C. Witthoeft, J. S. Adams, S. R. Bandler, S. Beaumont, J. A. Chervenak, M. E. Eckart, F. M. Finkbeiner, R. L. Kelley, C. A. Kilbourne, A. R. Miniussi, F. S. Porter, K. Sakai, S. J. Smith, N. A. Wakeham, E. J. Wassell

December 7, 2022

19th International Workshop on Low Temperature Detectors (LTD19)
Virtual (Boulder host), CO, United States
July 19, 2021 through July 29, 2021

Disclaimer

LLNL-CONF-843036

Correcting energy estimation errors due to finite sampling of transition edge sensor data

M. C. Witthoeft[1,2] • J. S. Adams[1,3] • S. R. Bandler[1]
S. Beaumont[1,3] • J. A. Chervenak[1] • M. E. Eckart[4]
F. M. Finkbeiner[1,5] • R. L. Kelley[1] • C. A. Kilbourne[1]
A. R. Miniussi[1,3] • F. S. Porter[1] • K. Sakai[1,3] • S. J. Smith[1]
N. A. Wakeham[1,3] • E. J. Wassell[1,6]

[1]*NASA Goddard Space Flight Center, Greenbelt, MD 20771 USA*
[2]*ADNET Systems, Inc., Bethesda, MD USA*
[3]*Center for Research and Exploration in Space Science and Technology, University of Maryland Baltimore County, Baltimore, MD, USA*
[4]*Lawrence Livermore National Laboratory, 7000 East Avenue, Livermore, CA 94550, USA*
[5]*Sigma Space Corp., Lanham, MD, USA*
[6]*KBRWyle, Lexington Park, MD, USA*

Abstract We are developing transition edge sensor (TES) microcalorimeters for the X-ray Integral Field Unit (X-IFU) on-board ESA's Athena space telescope. These detectors will be read out using Time-Domain-Multiplexing (TDM). Due to the limitations on bandwidth and dynamic range of the readout, the optimally filtered pulse heights of the measured x-ray signals suffer from a nonlinear variation with the exact photon arrival time relative to the sampling points. The shape and magnitude of this variation depend on the photon energy. We describe a method to characterize this energy-dependent variation with few parameters, which can then be interpolated to correct event energies across the whole spectrum. We implement our method on measurements from 200 pixels in a prototype X-IFU kilo-pixel array read out using 8-column x 32-row TDM. We show that the interpolation errors between calibration points, over the energy range 4-12 keV, can be made sufficiently small that they do not adversely impact the measured energy resolution across the full spectral range.

Keywords Transition-edge sensor • Athena space telescope • X-ray spectroscopy

Corresponding author email michael.c.witthoeft@nasa.gov

Declarations

- **Funding** Part of this work was performed under the auspices of the U.S. Department of Energy by Lawrence Livermore National Laboratory under Contract DE-AC52-07NA27344.
- **Conflicts of interest/Competing interests** The authors have no conflicts of interest to declare that are relevant to the content of this article.
- **Availability of data and material** The datasets generated and analyzed during the current study are available from the corresponding author on reasonable request.
- **Code availability** Computations were performed using custom code.
- **Authors' contributions** All authors contributed to the study conception and design. Data collection was performed by SJS and the analysis was performed by MCW.
- **Ethics approval** Not applicable
- **Consent to participate** Not applicable
- **Consent for publication** Not applicable

1 Introduction

The Advanced Telescope for High Energy Astrophysics (Athena) is an X-ray telescope selected by ESA to be launched in the early 2030's [1]. The X-ray Integral Field Unit (X-IFU) is an instrument on Athena that will provide high-resolution, imaging spectroscopy. The X-IFU will have a bandpass of 0.2-12 keV and a full-width-at-half-maximum energy resolution of ΔE_{FWHM} = 2.5 eV for energies up 7 keV. The X-IFU will use a microcalorimeter array of 3168 Mo/Au transition-edge sensors (TESs), under development at NASA Goddard Space Flight Center [2], which will be read-out using time division multiplexing (TDM) developed at NIST (Boulder, CO) [3,4]. We have recently reported on the broad-band performance of prototype kilo-pixel array in which ~200 pixels were readout using 8-column x 32-row TDM. This spectrometer demonstrated ΔE_{FWHM} = (2.16±0.006) eV at a photon energy of 6.9 keV, meeting the X-IFU requirements [5].

We are now working on methods to calibrate the instrument to simultaneously meet the energy scale and energy resolution requirements. One aspect of the calibration is correcting for biases in the energy estimates that arise due to the random arrival phase of photons relative to the digital sampling of the data stream [6,7,8] which primarily affect the energy resolution. This error is a function of the photon energy requiring calibration over the full energy range of the instrument. One method [8] developed using simulated photons consists of constructing a 2D calibration curve in energy and arrival time space using a polynomial fit. With real events, we have found that polynomials provide an unreliable fit to the arrival time variation of energy. Therefore, in this paper, we describe an approach to characterize it with a more complex parameterized function, which can then be interpolated to improve the energy resolution across the full spectrum.

2 Optimal Filtering and Arrival Time Correction

The arrival time induced energy error is a direct consequence of applying an optimal filter to pulse events whose exact arrival time is unknown. The optimal filter is constructed in the frequency domain from the measured average pulse shape divided by the measured average noise power [7]. The pulse height of an event is then computed as the dot product of the optimal filter with the event record in the time domain. If every measured event was in perfect phase with the template, no pulse height correction would be required. However, the finite sample rate of the digital readout (limited by the bandwidth of the system) results in a distribution of arrival times with respect to the digital sampling. To account for this, we compute multiple dot products where the optimal filter has been shifted by an integral number of samples. Using the shift yielding the largest dot product, and the two adjacent shifts (typically -1, 0, +1 samples), we fit a parabola and take the peak as the measured pulse height of the event. The location of the peak relative to the nearest whole sample is the lagphase. There is some error in this measurement because the shape of the pulse height vs lagphase curve is not perfectly parabolic. This biases the energy estimate and degrades the resolution if not corrected. If the error was only caused by finite digital sampling, then the underlying dependency may be more easily modelled and predicted. However, in TDM, the limited dynamic range of the digital feedback loop means that the linear range of the SQUID amplifier may be exceeded between successive samples of the pulse. The size of the excursion depends on the photon energy and the exact arrival time with respect to the sample rate. This introduces additional non-linearities in the first few samples of the pulse that can greatly complicate the resulting energy biases. Thus, we turn to empirical methods to correct the event pulse heights. Since the arrival time errors are pre-dominantly associated within the highest frequencies of the measured signal, the magnitude of the error can be mitigated by bandwidth limiting the optimal filter, but at the expense of a reduced signal-to-noise ratio. Having a separate method to characterize and correct for the energy error helps reduce how much bandwidth limiting is needed.

Our approach for correcting this error is to compute an empirical function, f(x), that captures the arrival time variation, such that

$E_{measured}(x) = E_{actual}\ f(x)$ (1)

where x is lagphase. Once we determine f(x) for each pixel, we can divide our event energies ($E_{measured}$) by f(x) evaluated at the event lagphase to obtain the corrected energy (E_{actual}). Note that energy in this context can be the real energy or any other energy analog (e.g., pulse height). We obtain f(x) by separating events from a single calibration line into lagphase bins and then fit a theoretical line shape to the pulse height histogram of the events in each bin. The resulting line position as a function of lagphase is normalized by the fiducial line position to obtain f(x). Since the shape and magnitude of the energy variation with lagphase is itself energy dependent, this method only works well for correcting events at a single energy. In [5], a series of independent measurements were carried out at 5 different fiducial $K\alpha$ line energies over the range 4.5 -12 keV. As such, we could use this approach correct the arrival time energy bias for each data set independently, and thus demonstrate the best achievable ΔE_{FWHM} at each line. However, more generally for an instrument such as X-IFU, photons will be simultaneously measured over a wide range of energies, thus we must characterize the shape and magnitude over the full bandpass in order to properly calibrate the instrument.

3 Characterization of the broad band lagphase error

Measurements for this study are carried out on ~200 pixels in a prototype X-IFU kilo-pixel array, read out using 8-column x 32-row TDM [5]. X-rays are generated using a rotating-target-source (RTS) that consists of a bright continuum x-ray source that illuminates a series of target materials mounted on a rotating wheel (high purity metal disks of Sc, Ti, V, Cr, Mn, Fe, Co, Ni, Cu, Zn and Ge, and a KBr crystal). By rotating each target into the primary x-ray beam we can generate fluorescent $K\alpha$ and $K\beta$ lines from each target in turn. The count-rate per pixel ranged from 0.4 to 2.0 cps/pixel, depending upon the target. The hold time on each target was tuned such that the total number of events measured was approximately equal for all targets during one full rotation period (346s). Data are measured continuously over a 60 hr period, which provides ~40M x-ray events. After cuts are made to reject double-pulse and crosstalk events, there are ~7000 events in each $K\alpha$ complex for each pixel. Corrections are made to each pixel individually to account for drifts in the detector gains over time (of typically a few eV).

Correcting energy estimation errors due to finite sampling of transition edge sensor data

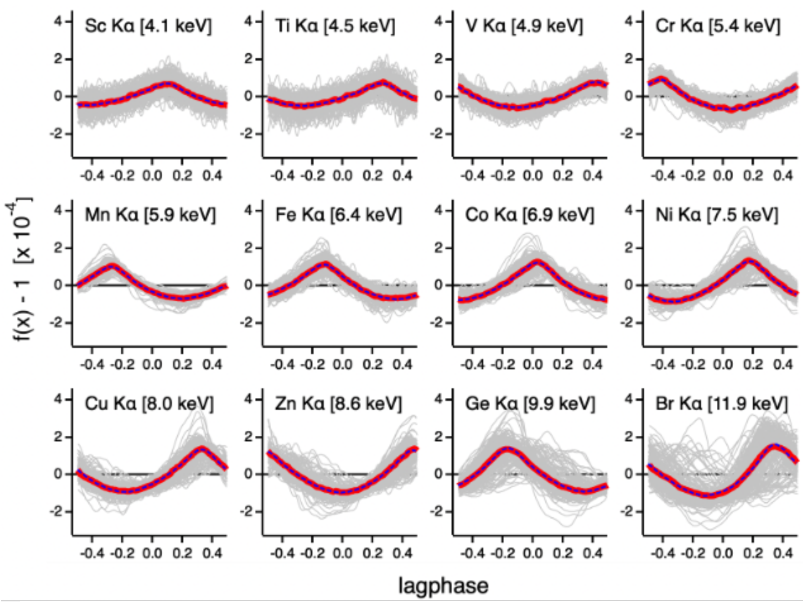

Figure 1 Arrival-time correction factors as a function of lagphase for each pixel and for each calibration line (*thin gray curves*), the correction factor obtained by combining events from all pixels (*thick red curve*), and the parameterized fit to the combined-pixel correction factor (*thin, dashed blue curve*). (Color figure online)

In Fig. 1 we show the arrival time variation as a function of lagphase, f(x), for the 12 Kα lines for all pixels in the array (gray curves). The shape of the variation is similar in form for each line, but there is a clear energy-dependence to the amplitude and position of the peak. The differences in f(x) between pixels can be attributed to the effects of statistics as well as physical differences between the pixels. To reduce the effect of statistics, we construct an f(x) using the combined events over the whole array (shown as the red curve in Fig. 1). Note that we cannot simply combine all events together in pulse-height space due to the difference in energy scales between pixels, so, we first compute and apply a gain scale to our data. With improved statistics, these curves are much smoother and can be more easily parameterized. We use an empirical fit to each curve, $g(x-x_s)$ of the form

$$g(x) = 1 + B + A\,[2.5\,L(x) + \cos(2\pi x)] \qquad (2)$$

where

$$L(x) = \frac{1-q^2/4}{1+\frac{x}{\gamma}\left(\frac{x}{\gamma}+q\right)}\,. \qquad (3)$$

The parameters of this fit are x_s – location of the peak, B – vertical shift, A – amplitude, g – Lorentzian width, and q – Lorentzian skew. In Fig. 2, we show how the fitted parameters depend on energy. We found that the Lorentzian width was largely independent of energy, so we fix it to be constant. To ease interpolation over energy, we smooth each parameter by fitting a polynomial function. The fits are most sensitive to the x_s parameter, so it is smoothed first followed by a refitting and smoothing of the other parameters (blue curves in Fig. 2). Figure 3 shows the parameterized arrival time correction curves using the unsmoothed and smoothed parameters for the highest-energy lines to illustrate the good agreement between the two. With the smoothed parameters, we can construct an arrival time variation vs lagphase curve at any energy using linear interpolation. We then use Eq. (1) to correct event energies across the entire spectrum. The resulting energy histograms for each pixel are added together and then fit with the assumed line profile for each Kα complex to determine the Gaussian energy response with the best-fit value of the ΔE_{FWHM}. In Fig. 4 we show ΔE_{FWHM} for each calibration line using the uncorrected energy (red circles) compared with the corrected energy using the smoothed parameters (blue square) and energies corrected using the pixel-dependent (gray) curves from Fig. 1 (purple diamonds). While there is a clear improvement in ΔE_{FWHM}, particularly at high energies where the arrival time error is the largest, the pixel-dependent nature of the arrival time variation is seen to limit the effectiveness of the combined-pixel derived parameters. The dependency of ΔE_{FWHM} on energy is a result of several factors that include: the intrinsic detector non-linearity, residual cross-talk (not removed by standard data cuts) and uncertainties in the theoretical line shapes of the Kα complexes. Note that the per-pixel count-rates are up to x4 larger than the measurements reported in ref [5]. Consequently, the effect of residual cross-talk is worse, and degrades the measured ΔE_{FWHM} above the best achievable performance from ref [5].

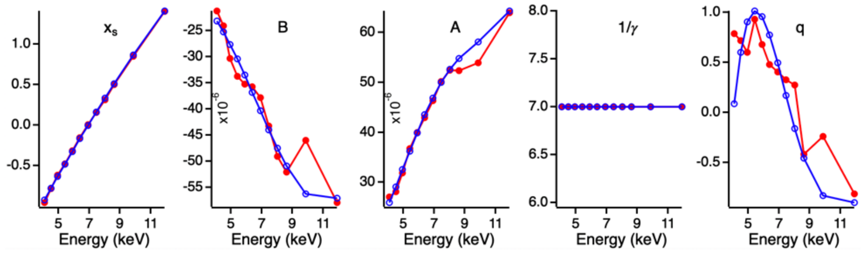

Figure 2 Fitted lagphase correction parameters versus energy of the calibration line – unsmoothed (*red curve with filled circles*) and smoothed (*blue curve with open circles*). (Color figure online).

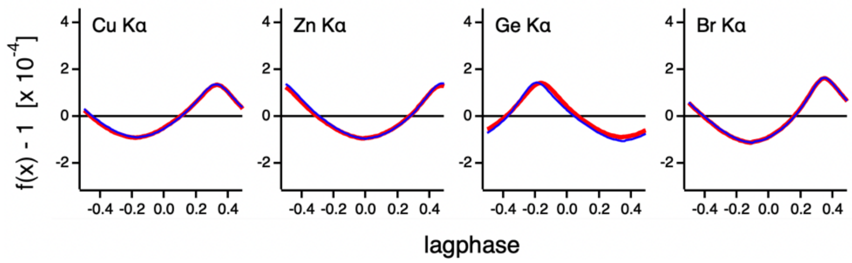

Figure 3 Comparison of lagphase variation fits using unsmoothed (*thick, red*) and smoothed (*thin, blue*) parameters for the 4 highest energy calibration lines. (Color figure online)

To recover the pixel dependence of the arrival time variation, we use our parameterized function to fit the per-pixel (gray) curves in Fig. 1. However, poor statistics makes blind fitting unreliable. So, we perform the fits in an iterative way starting with the smoothed parameters from Fig. 2. The resulting pixel-dependent parameters are shown in Fig. 5. The line resolutions resulting from these parameters (green triangles in Fig. 4) show agreement within 0.25 eV RSS (residual sum of squares) with the single-line corrections (purple diamonds) at energies below 7 keV increasing to 0.5 eV RSS at 12 keV indicating that the smoothed, pixel-dependent parameters capture the bulk of the arrival time variation.

We next investigate how reliably these parameters can be interpolated across the full energy range by computing parameters for each of our 12 Kα lines using linear interpolation of the parameters from the two neighboring lines. For the lowest/highest energy lines, we use linear extrapolation. We then compare the corrected energies from the interpolated parameters with the smoothed parameters for that line. With the exception of the two highest-energy lines, we find that interpolation only degrades the resolution by at most 0.1 eV RSS. For the Ge Ka line we lose 0.24 eV RSS due to the parameter smoothing effects and for the Br Ka line, a loss of 1 eV RSS is due to extrapolation. Given that these interpolations are being performed over artificially wide gaps since we are removing calibration lines, we expect the true loss of resolution due to interpolation to be better than reported here.

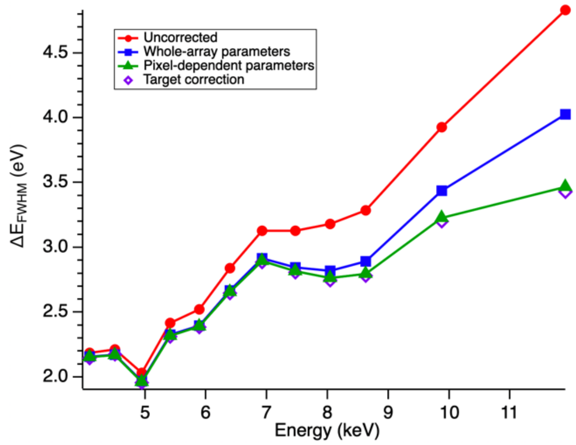

Figure 4 Fitted ΔE_{FWHM} of the 12 Kα lines using the uncorrected event energies (*red circles*), energies corrected using the pixel-dependent factors from Fig. 1 (*open purple diamonds*), energies corrected using the combined-pixel, smoothed parameters from Fig. 2 (*blue squares*), and energies corrected using the pixel-dependent, smoothed parameters (*green triangles*). All statistical fit errors are within 0.01 eV. (Color figure online)

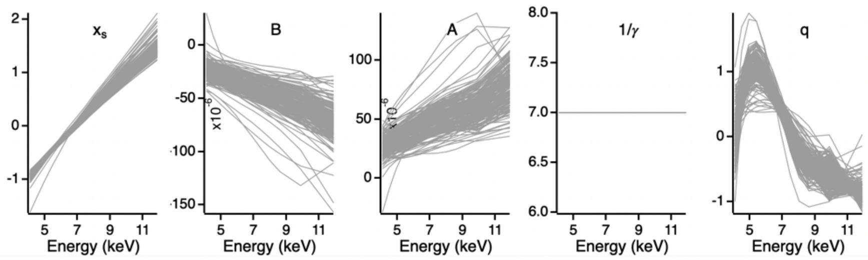

Figure 5 Pixel-dependent lagphase correction parameters. The $1/\gamma$ parameter has been frozen to a value of 7.

4 Conclusion

Correcting energy estimation errors due to finite sampling of transition edge sensor data

The X-IFU instrument on the Athena telescope will be read out using TDM which can suffer from an energy error dependent on the exact arrival time of the photons relative to the sampling points. We have presented a parameterized function which accurately captures the energy error as a function of lagphase. By interpolating these parameters over energy, we have demonstrated that we can correct for the error across the entire spectrum at the nearly the same accuracy as single-energy correction methods.

In the future, we will continue to refine the parameterized function for fitting the energy variation with arrival time and better automate the calibration procedure. We are also investigating ways to reduce the magnitude of the variation during construction of the optimal filter with minimal loss of NEP.

Acknowledgements

Part of this work was performed under the auspices of the U.S. Department of Energy by Lawrence Livermore National Laboratory under Contract DE-AC52-07NA27344.

References

1. D. Barret et al., “The athena X-ray integral field unit (X-IFU),” in Proc. SPIE Space Telescopes Instrum. Ultraviolet Gamma Ray, 2016, Art. no. 99052F.
2. S. J. Smith et al., “Transition-edge sensor pixel parameter design of the microcalorimeter array for the X-ray integral field unit on Athena,” in Proc. vol. 9905, Space Telescopes Instrum. Ultraviolet Gamma Ray, 2016, Art. no. 99052H.
3. W. B. Doriese et al., “Developments in time-division multiplexing of X-ray transition-edge sensors,” J. Low Temp. Phys., vol. 184, pp. 389–395, 2016.
4. M. Durkin et al., "Mitigation of Finite Bandwidth Effects in Time-Division-Multiplexed SQUID Readout of TES Arrays," in *IEEE Transactions on Applied Superconductivity*, vol. 31, no. 5, pp. 1-5, Aug. 2021, Art no. 1600905, doi: 10.1109/TASC.2021.3065279.
5. S. J. Smith et al., "Performance of a Broad-Band, High-Resolution, Transition-Edge Sensor Spectrometer for X-ray Astrophysics," in *IEEE Transactions on Applied Superconductivity*, vol. 31, no. 5, pp. 1-6, Aug. 2021, Art no. 2100806, doi: 10.1109/TASC.2021.3061918.
6. J.W. Fowler et al., “The practice of pulse processing,” J. Low Temp. Phys., vol. 184, pp. 374–381, 2016. doi: 10.1007/s10909-015-1380-0

7. J. S. Adams et al., "Real - Time Data Processing for X - Ray Spectroscopy", *AIP Conference Proceedings*, vol. 1185, 274 (2009); https://doi.org/10.1063/1.3292331
8. M.T. Ceballos et al., "Jitter and Readout Sampling Frequency Impact on the Athena/X-IFU Performance", *Astronomical Data Analysis Software and Systems XXVIII ASP Conference Series*, Vol. 523 P.J. Teuben, M.W. Pound, B.A. Thomas, and E.M. Warner, eds. 2019.

Grayscale figures:

Fig 1

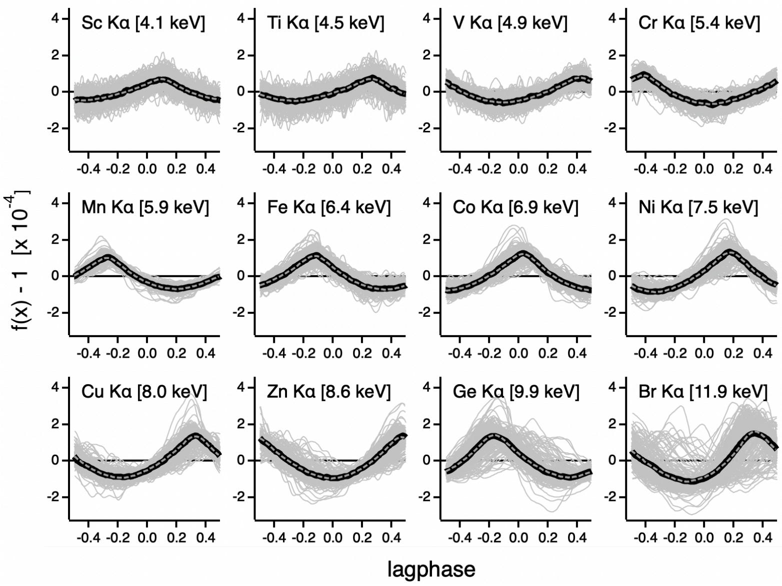

Fig2

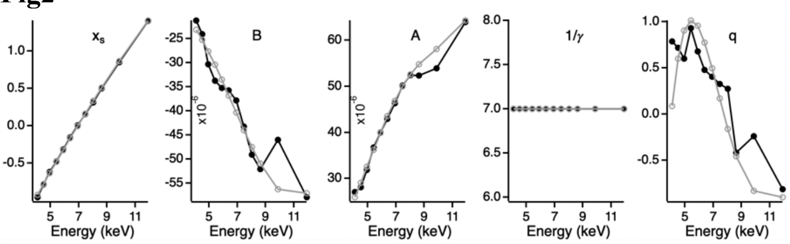

Correcting energy estimation errors due to finite sampling of transition edge sensor data

Fig 3

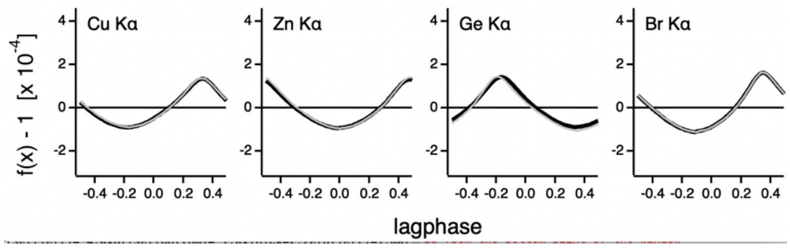

Fig 4